

LETTER TO THE EDITOR

# Discovery of a new M32-like “Compact Elliptical” galaxy in the halo of the Abell 496 cD galaxy <sup>★</sup>

I. Chilingarian<sup>1,2</sup>, V. Cayatte<sup>3</sup>, L. Chemin<sup>4</sup>, F. Durret<sup>5,1</sup>, T. F. Laganá<sup>6</sup>, C. Adami<sup>7</sup>, and E. Slezak<sup>8</sup>

<sup>1</sup> Observatoire de Paris-Meudon, LERMA, UMR 8112, 61 Av. de l’Observatoire, Paris, 75014, France

<sup>2</sup> Sternberg Astronomical Institute, Moscow State University, 13 Universitetski prospect, 119992, Moscow, Russia

<sup>3</sup> Observatoire de Paris-Meudon, LUTH, UMR 8102, 5 pl. Jules Janssen, Meudon, 92195, France

<sup>4</sup> Observatoire de Paris-Meudon, GEPI, UMR 8111, 5 pl. Jules Janssen, Meudon, 92195, France

<sup>5</sup> Institut d’Astrophysique de Paris, CNRS, UMR 7095, Université Pierre et Marie Curie, 98bis Bd Arago, 75014 Paris, France

<sup>6</sup> Instituto de Astronomia, Geofísica e C. Atmosf./USP, R. do Matão 1226, 05508-090 São Paulo/SP, Brazil

<sup>7</sup> Laboratoire d’Astrophysique de Marseille, UMR 6110, Traverse du Siphon, 13012 Marseille, France

<sup>8</sup> Observatoire de la Côte d’Azur, Laboratoire Cassiopée, UMR 6202, BP 4229, 06304 Nice Cedex 4, France

Received March 01, 2007; accepted March 13, 2007; in original form February 13, 2007

## ABSTRACT

**Aims.** “Compact ellipticals” are so rare that a search for M32 analogs is needed to ensure the very existence of this class.

**Methods.** We report here the discovery of A496cE, a M32 twin in the cluster Abell 496, located in the halo of the central cD.

**Results.** Based on CFHT and HST imaging we show that the light profile of A496cE requires a two component fit: a Sérsic bulge and an exponential disc. The spectrum of A496cE obtained with the ESO-VLT FLAMES/Giraffe spectrograph can be fit by a stellar synthesis spectrum dominated by old stars, with high values of [Mg/Fe] and velocity dispersion.

**Conclusions.** The capture of A496cE by the cD galaxy and tidal stripping of most of its disc are briefly discussed.

**Key words.** evolution of galaxies – kinematics – stellar populations – dwarf galaxies

## 1. Introduction

Compact elliptical galaxies are known to be high surface brightness low-luminosity objects like the prototype of this class, M 32, satellite of the Andromeda galaxy. Compared to dwarf ellipticals of same absolute magnitude, the effective surface brightness of M 32 is about 100 times higher and its effective radius is 10 times smaller (Graham 2002). Presently, only five objects belonging to the class of “compact elliptical” galaxies (cE) are known; the four other objects are NGC 4486B (in the vicinity of M 87, the Virgo cluster cD), NGC 5846A (a close satellite of the giant elliptical galaxy NGC 5846), and two objects in the Abell 1689 cluster (Mieske et al. 2005). These extremely rare galaxies are thought to be generated by tidal stripping of more massive galaxies (Nieto & Prugniel 1987, Bekki et al. 2001, Choi et al. 2002), but how such a high stellar surface density can be put in the central part of the galaxy is not entirely clear. The structural parameters of M 32 derived by Graham (2002) from the light profile include a bulge and a low surface brightness disc, indicating that the precursor could be an early type disc galaxy. The evolution in the past of the prototypical cE is however still a matter of debate (see Mieske et al. 2005) and several observational projects aimed at searching for cE galaxies

Send offprint requests to: Igor Chilingarian e-mail: igor.chilingarian@obspm.fr

<sup>★</sup> Based on observations obtained at the Canada-France-Hawaii Telescope (program 03BF12) which is operated by the National Research Council of Canada, the Institut des Sciences de l’Univers of the Centre National de la Recherche Scientifique and the University of Hawaii. Also based on ESO VLT data (program 074.A-0533), and on HST archive data (proposals 5121 and 8683).

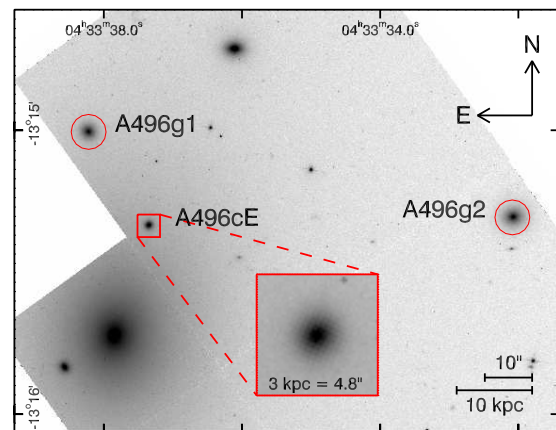


**Fig. 1.** HST WFPC2 image of the central region of Abell 496 (filter F702W). The objects discussed in this *Letter* are labeled.

were conducted until now with no success (Drinkwater & Gregg 1998, Ziegler & Bender 1998).

In this *Letter* we report the discovery of the sixth “compact elliptical” galaxy in the cluster Abell 496. We present results based on the analysis of high-resolution spectroscopic data ( $R=7000$  in the 5000–5800 Å range) obtained with FLAMES/Giraffe (multi-object “MEDUSA” mode) at ESO VLT UT2 in the fall of 2004, combined with a photometric study based on HST WFPC2 direct images in three filters: F555W, F702W, and F814W available through the HST archive. The dis-

covery has been made from deep ground-based  $u^* g' r' i'$  imaging conducted at CFHT with Megacam in the fall of 2003 and dedicated to obtain morphological and structural properties of dwarf early type galaxies in Abell 496. Detailed informations on spectroscopic and photometric observations as well as data reduction will be provided in a forthcoming paper discussing the whole sample of galaxies.

For the Abell 496 cluster we adopt the distance modulus 35.70 and spatial scale  $0.627 \text{ kpc arcsec}^{-1}$ , assuming  $H_0 = 73 \text{ km s}^{-1}$ ,  $\Omega_M = 0.27$ , and  $\Omega_\Lambda = 0.73$ . All the photometric measurements discussed in this Letter are corrected for Galactic absorption according to Schlegel et al. (1998), and redshift effect ( $K$ -correction) assuming an early-type galaxy spectrum. A cosmological surface brightness dimming correction has been applied with the cluster velocity, corrected for infall of the Local Group towards Virgo taken equal to  $9707 \text{ km s}^{-1}$ .

## 2. Properties of the newly discovered object

The galaxy is listed in HyperLeda<sup>1</sup> as PGC 3084811 (Paturel et al. 2003). However, this name cannot be resolved by other public astronomical databases (NED, SIMBAD), therefore we adopt the IAU recommended name, ACO496J043337.35-131520.2 and will refer to it hereafter as “A496cE”.

A496cE is located 22 arcsec (14 kpc in projected distance) from the cluster centre; it appears in projection on the outer parts of the central cD galaxy (see Fig. 1). The background (i.e. the cD halo) has been subtracted from the HST images using a multiscale wavelet analysis and reconstruction technique described e.g. by Adami et al. 2005. The cD halo surface brightness at the region where A496cE resides is about  $24 \text{ mag arcsec}^{-2}$  in the  $B$  band and has a significant gradient, therefore correct background estimation is crucial for the surface photometry of A496cE. Elliptical isophotes with free central position, ellipticity and position angle have been fitted to the images of A496cE using the IRAF ELLIPSE task. On the  $r'$  image, the position angle changes notably and the ellipticity rises from about 0.05 to 0.1 between 1.8 and 2.6 arcsec.

We have combined the HST light profiles for the inner part of the galaxy ( $radius < 3.5 \text{ arcsec}$ ) with the deeper  $r'$  band CFHT photometry for the outer parts ( $radius > 3.5 \text{ arcsec}$ ), where the seeing (FWHM=0.8 arcsec) does not play an important role. The empirical normalization factor for the  $r'$  profile has been derived from the best match of the two profiles between 2 and 4 arcsec.

We have fit the 1-dimensional surface brightness profile using both a Sérsic and a Sérsic + exponential disc model (see Graham 2002 and Graham & Guzmán 2003) with a free constant background level within 10 arcsec from the galaxy centre. As in the case of M 32 (Graham 2002), a single-component Sérsic profile does not fit accurately the light profile and an exponential disc is needed. Fig. 2 and Table 1 present the surface brightness profile of A496cE and the best-fitting results of the photometric decomposition of the profile.

An unsharp masking technique with elliptical blurring (Lisker et al. 2006), shown to be very sensitive to the presence of possible embedded structures, reveals no structures either on HST or on CFHT images.

We have built F555W-F702W and F555W-F814W colour maps using the Voronoi adaptive binning technique (Cappellari & Copin 2003) to achieve minimal signal-to-noise ratios of 20 per bin in the F814W image and 40 in F702W. No colour gradient is detected. However, this should not be considered as a

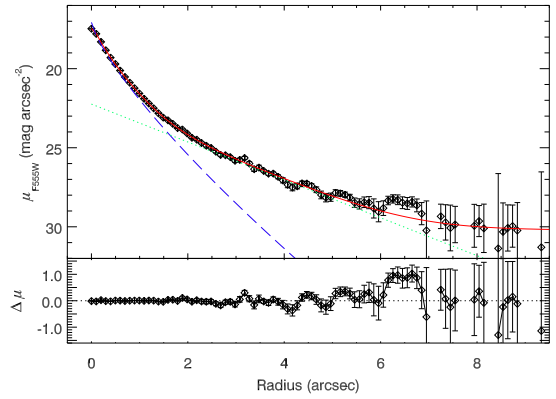


**Fig. 2.** Best fitting two-component Sérsic+disc profile overplotted on the composite light profile (F555 and  $r'$ ). Bulge and disc components are shown as dash-dotted blue and dashed green lines respectively.

**Table 1.** Global parameters (luminosity, radial velocity, central velocity dispersion) and best-fitting parameters for the one-component (Sérsic) or two-component model (Sérsic+disc) of the light profiles of A496cE, A496g1, and A496g2 in  $B$  band. Data for M 32 are taken from van der Marel et al. (1998), Graham (2002), and for NGC 4486B from Ferrarese et al. (2006) and HyperLeda.

	A496cE	A496g1	A496g2	M 32	N4486B
$M_{B,tot}$	-16.79	-17.32	-17.91	-15.85	-16.63
$v \text{ km/s}$	$9747 \pm 1$	$10286 \pm 3$	$9948 \pm 1$	$-197 \pm 15$	$1557 \pm 35$
$\sigma_0 \text{ km/s}$	$104 \pm 2$	$145 \pm 3$	$79 \pm 1$	$76 \pm 10$	$170 \pm 4$
$M_{B,b}$	-16.60	-17.32	-17.91	-15.34	-16.63
$R_{e,b} \text{ kpc}$	0.24	0.66	0.96	0.10	0.18
$\mu_{0,b}$	17.37	18.70	17.79	16.31	14.00
$n_b$	1.29	1.35	1.94	1.5	2.73
$\mu_e$	19.82	21.30	21.65	19.23	19.58
$\langle \mu \rangle_e$	18.00	20.44	20.63	18.34	18.39
$M_{B,d}$	-14.80	n/a	n/a	-14.78	n/a
$R_{e,d} \text{ kpc}$	0.92	n/a	n/a	0.84	n/a
$\mu_{0,d}$	22.55	n/a	n/a	22.28	n/a

certain evidence for the uniform distribution of stellar population parameters with radius. For instance, for M 32 the effects of age and metallicity gradients on the  $V - I$  colour exactly compensate each other, resulting in a flat colour profile (Rose et al. 2005).

We have analysed the spectrum of A496cE using the novel stellar population fitting technique described in detail in Chilingarian (2006) and Chilingarian et al. (2007). By fitting the spectrum with high-resolution models of simple stellar populations (SSP) computed with PEGASE.HR (Le Borgne et al. 2004), we are able to extract simultaneously stellar kinematics:  $v$ ,  $\sigma$ , and stellar population parameters such as SSP-equivalent age and metallicity. Although some template mismatch is seen due to the supersolar  $[\alpha/Fe]$  in A496cE, the quality of the fit is rather good ( $\chi^2/DOF = 1.6$ ).

We have obtained the  $\alpha/Fe$  abundance ratio of the stellar population by measuring the following absorption line-strength indices (Worthey et al. 1994):  $Mgb$ ,  $Fe_{5270}$ , and  $Fe_{5335}$  using the  $\alpha$ -enhanced models by Thomas et al. (2003). The kinematical parameters are given in Table 1 and those of the stellar populations in Table 2. A496cE has a rather high velocity dispersion for its luminosity. It resides above the sequence of ellip-

<sup>1</sup> <http://leda.univ-lyon1.fr/>

**Table 2.** Stellar population parameters of A496cE, A496g1, and A496g2 compared to M 32 and NGC 4486B (Sánchez-Blázquez et al. 2006). Comma-separated values for M 32 correspond to the parameters at the core and at one effective radius as given by Rose et al. (2005).

	$t$ , Gyr	$Z$ , dex	[Mg/Fe]
A496cE	$16.4 \pm 1.9$	$-0.04 \pm 0.02$	$0.19 \pm 0.07$
A496g1	$15.3 \pm 2.8$	$-0.19 \pm 0.03$	$0.43 \pm 0.09$
A496g2	$13.1 \pm 2.0$	$-0.43 \pm 0.03$	$0.28 \pm 0.08$
M 32	4.0, 7.0	0.00, -0.25	-0.25, -0.08
N4486B	9.5	0.4	0.3

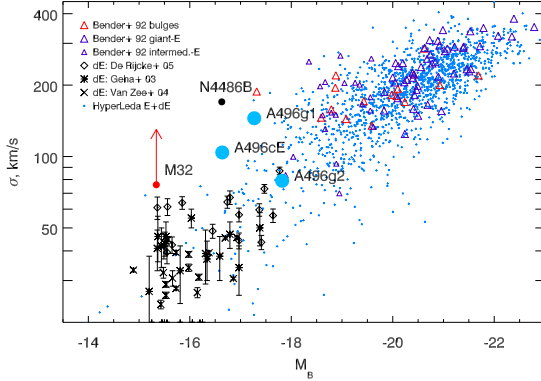


**Fig. 3.** Faber–Jackson relation for ellipticals and bulges of disc galaxies. Giant and intermediate-luminosity ellipticals are in blue, bulges of disc galaxies in red, dwarf ellipticals and lenticulars in black. The upper end of the arrow representing M 32 corresponds to the HST STIS measurements (Joseph et al. 2001), and the filled circle represents the value obtained from earlier HST FOS data (van der Marel et al. 1998), which was in agreement with more recent ground-based observations.

tical galaxies on the Faber–Jackson (1976) relation, shown in Fig. 3, presenting a compilation of data for dwarf (Geha et al. 2003; van Zee et al. 2004; De Rijcke et al. 2005), intermediate luminosity, and giant elliptical galaxies and bulges of bright lenticulars (Bender et al. 1992). Due to the aperture size of the FLAMES/Giraffe fibre our velocity dispersion for A496cE nearly corresponds to the effective velocity dispersion and the central value is probably significantly higher. The properties of A496cE, such as metallicity and Mg/Fe ratio are similar to those of bulges of moderate-luminosity lenticulars and spirals. The age and metallicity of A496cE correspond to a stellar mass-to-light ratio  $(M/L)_{*,B} = 19 \pm 2 (M/L)_{\odot}$  (value for the PEGASE.HR SSP computed with Salpeter IMF). Thus, the derived stellar mass of A496cE is  $(1.7 \pm 0.4) \cdot 10^{10} M_{\odot}$ .

### 3. Discussion

#### 3.1. Comparison with other E, dE, and cE galaxies

The very small effective radius, about 250 pc, high mean surface brightness,  $\mu_{Be} = 19.60 \text{ mag arcsec}^{-2}$ , and dwarf luminosity ( $M_B = -16.96 \text{ mag}$ ) put the bulge of A496cE on the continuation of the sequence of giant ellipticals and bulges in the Kormendy (Kormendy 1977) and  $M_B - \mu_{\text{eff}}$  diagrams toward small effective radii and fainter luminosities. Fig. 4 presents the updated versions of Figs. 9a,g from Graham & Guzmán (2003): absolute  $B$  magnitude and effective radius  $R_e$  versus mean  $B$  sur-

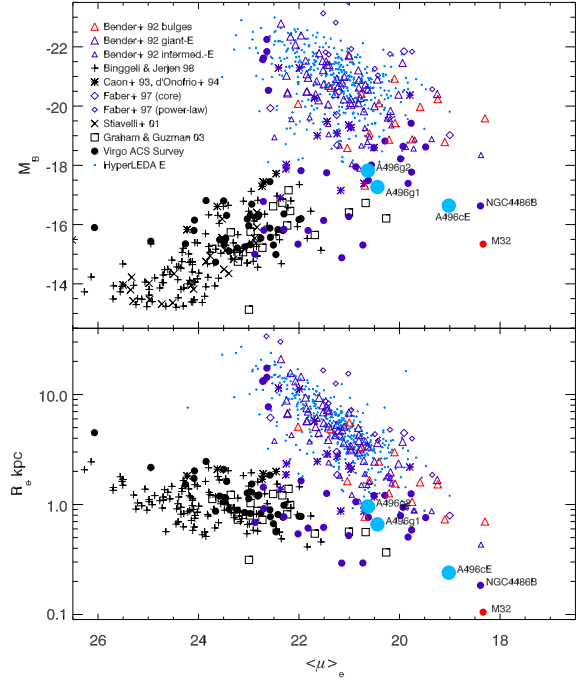


**Fig. 4.** Structural properties of elliptical galaxies and bulges. Giant and intermediate-luminosity ellipticals, power-law and core galaxies are shown in blue, bulges of disc galaxies in red, dwarf ellipticals and lenticulars in black. We keep the original morphological classification (E / dE) for the data points coming from the Virgo Cluster ACS Survey, Caon et al. (1993), and D’Onofrio et al. (1994), therefore they appear both in blue and black.

face brightness within effective radius  $\langle \mu \rangle_e$ . The plot contains only data for elliptical galaxies and bulges of lenticulars/spirals (where bulge/disc decomposition has been made in the original sources), all integrated measurements for S galaxies have been excluded. Data in computer-readable format for dE and E galaxies from Binggeli & Jerjen (1998), Caon et al. (1993), D’Onofrio et al. (1994), Faber et al. (1997), Graham & Guzmán (2003), Stiavelli et al. (2001) and homogenization algorithms for these datasets have been kindly provided by A. Graham. We also included: photometric parameters of E and dE/dS0 galaxies from the Virgo Cluster ACS Survey (Ferrarese et al. 2006), photometric data on giant, intermediate elliptical galaxies and bulges of spirals and lenticulars from Bender et al. (1992), photometric parameters of the Sérsic component of M 32 (Graham 2002), and data for 430 elliptical galaxies from the HyperLeda database, with radial velocities below  $10000 \text{ km s}^{-1}$  and brighter than  $M_B = -18.0 \text{ mag}$ . All the measurements are corrected for Galactic absorption, cosmological dimming, K-correction, and converted into  $B$  band according to Fukugita et al. (1995) assuming an elliptical galaxy SED.

Reflecting structural properties of elliptical galaxies, giants and dwarfs reside in different regions of these diagrams. The sequence formed by giant elliptical galaxies and bulges of spirals is clearly extended towards smaller effective radii / higher surface brightnesses by M 32 and NGC 4486B. A496cE resides very close to NGC 4486B in both plots. Thus, we can conclude that the structural properties of the A496cE bulge resemble those of elliptical galaxies and bulges of spirals and lenticulars. However

the bulges of M 32 and A496cE lie in a region where no other object is found, indicating that they differ from normal bulges.

We have chosen S0 galaxies from the sample of Sil'chenko (2006), with velocity dispersion and stellar population parameters coinciding with the values for A496cE: NGC 3098 ( $\sigma = 105 \text{ km s}^{-1}$ ,  $[\text{Fe}/\text{H}] = -0.2$ ,  $t = 10 \text{ Gyr}$ ), and NGC 4379 ( $\sigma = 108 \text{ km s}^{-1}$ ,  $[\text{Fe}/\text{H}] = 0.0$ ,  $t = 15 \text{ Gyr}$ ). Their  $B$  luminosities ( $M_B = -18.9, -18.6$ , HyperLeda) are about two magnitudes higher than that of A496cE. Assuming a bulge-to-disc ratio of 1:1 by mass for early-type galaxies, this implies that if the progenitor of A496cE was an intermediate-luminosity disc galaxy, with its disc completely stripped by harassment, it must have lost at least 2/3 of its bulge mass.

We now compare the properties of A496cE with two galaxies of our spectroscopic sample in the WFPC2 field: ACO496J043338.22-131500.7 and ACO496J043332.07-131518.1 (PGC 93410), hereafter A496g1 and A496g2 respectively. The light profile of A496g1 is well fitted with a single Sérsic component law. We can also fit the A496g2 profile with a single component model, though a faint disc in the external part may also be present, as discussed in a forthcoming paper. For both objects the effective radii are several times larger than for A496cE, while the luminosities do not differ strongly. The metallicity and velocity dispersion of A496g2 are not higher than expected for an object of such a luminosity, but the  $[\text{Mg}/\text{Fe}]$  ratio is very high, indicating a very short star formation period (see e.g. Matteucci, 1994). Gas might have been expelled by ram pressure, efficient in the central parts of rich clusters (see e.g. Abadi et al. 1999), so star formation was abruptly terminated.

For A496g1 the overall metallicity is  $\sim 0.2$  dex higher than expected for its luminosity, but the  $[\text{Mg}/\text{Fe}]$  ratio and velocity dispersion are exceptionally high (see Fig. 3), so this galaxy is closer to an intermediate-luminosity elliptical or S0 galaxy with  $M_B \approx -19$  mag. The old ages of the stellar populations of A496cE, A496g1, and A496g2 prove that none of these objects merged with galaxies having young stellar populations or star-formation during the last 10 Gyr, an indirect evidence for their habitation in the centre of Abell 496 since that epoch.

### 3.2. Possible origin of A496cE

The presence of an outer exponential disc in A496cE argues that this galaxy should not be considered as purely elliptical. Lisker et al. (2007) have proposed that only nucleated dwarf ellipticals follow the classical spheroid picture and a large number of dEs in Virgo could be shaped like thick discs and formed from mass loss from bigger infalling galaxies. However A496cE did not follow the same evolutionary path as the three peculiar subclasses of dwarfs described by Lisker et al., since its properties provide decisive evidence that this object is quite unique.

Block et al. (2006) have simulated a head-on collision of Andromeda with a low mass companion, now observed as M 32. Their numerical simulations show that a fraction of M 32 gets stripped on a timescale of a few  $10^7$  years. Under certain circumstances if the disc galaxy is stripped starting from its outer parts, the overall potential becomes shallower and the bulge may shrink, leading to a smaller object.

A496cE is observed very close to the cluster centre. If it has a short-period orbit partially immersed in the cD halo, consecutive passages should lead to a relatively fast and efficient stripping. The old stellar population of A496cE indicates that the main part of the disc was stripped long ago. But how could such an object

survive for about 10 Gyr very close to the cD galaxy without being accreted by it?

The two aspects that rule the processes of galaxy mergers are: (1) dynamical friction, decreasing the orbit size and causing an accreting object to pass closer and closer to the centre of the cluster; and (2) tidal forces, which can totally disrupt an object if it passes sufficiently close to the cD galaxy.

The bulge of A496cE is very compact and dense, thus it must be rather resistant to tidal disruption. Its exponential profile shows no evidence for truncation beyond the tidal radius of A496cE  $r_{tid} \sim 2 \text{ kpc}$ . We assume a pericentral distance  $d_p = 14 \text{ kpc}$ , i.e. that A496cE is passing near its pericentre now with an orbital plane orthogonal to the line of sight. This is possibly the case, because the radial velocity of A496cE differs from that of the cD by only  $100 \text{ km s}^{-1}$ . Assuming a mass of  $\sim 10^{13} M_\odot$  for the cD, the pericentral velocity is  $v \approx 2000 \text{ km s}^{-1}$ . The dynamical friction is  $\sim \frac{M^2 \rho}{v^2}$ . Given that A496cE is 4-6 times more massive (assuming the same dark matter fraction) than M 32 ( $\approx 3.0 \cdot 10^9 M_\odot$ ), the orbital velocity 10 times higher, and halo densities are comparable, the dynamical friction force is 3-4 times less efficient for A496cE than for M 32. Therefore, there is a good chance for A496cE to survive for billions of years in the central region of the cluster. Its progenitor must have lost a large fraction of its mass during the first passage in order to decrease significantly the dynamical friction effects. The high metallicity and supersolar  $[\text{Mg}/\text{Fe}]$  ratio are additional arguments for its massive progenitor origin.

**Acknowledgements.** Special thanks to Alister Graham and Françoise Combes for fruitful discussions and to the anonymous referee for his/her fast and careful report and useful suggestions. This *Letter* was inspired by the panel discussion "What is the relationship between compact ellipticals (such as M32) and more massive ellipticals" at IAU Symposium 241. We thank the CFHT team for service observing and the Terapix team for reducing our Megacam data. This paper has made use of the HST archive and of the NED and HyperLeda data bases. IC acknowledges support provided by the "HORIZON" project, INTAS YS Fellowship (04-83-3618) and bilateral Russian-Flemish grant RFBR-05-02-19805-MF-a.

## References

- Abadi M., Moore B., Bower R.G. 1999, MNRAS 308, 947
- Adami C., Slezak E., Durret F. et al. 2005, A&A 429, 39
- Bekki K., Couch W., Drinkwater M., Gregg M. 2001, ApJ, 557, L39
- Bender R., Burstein D., Faber S. M. 1992, ApJ 399, 462
- Binggeli B. & Jerjen H. 1998, A&A, 333, 17
- Block D. L., Bournaud F., Combes F. et al. 2006, Nature 443, 832
- Caon N., Capaccioli M., D'Onofrio M. 1993, MNRAS, 265, 1013
- Cappellari M. & Copin Y. 2003, MNRAS, 342, 345
- Chilingarian I. 2006, PhD Thesis, astro-ph/0611893
- Chilingarian I., Prugniel P., Sil'chenko O., Afanasiev V. 2007, MNRAS in press, astro-ph/0701842
- Choi P., Guhathakurta P., Johnston K. 2002, AJ, 124, 310
- De Rijcke S., Michielsen D., Dejonghe H., Zeilinger W. W., Hau G. K. T. 2005, A&A, 438, 491
- D'Onofrio M., Capaccioli M., Caon N. 1994, MNRAS 271, 523
- Drinkwater M. J. & Gregg M. D. 1998, MNRAS, 296, L15
- Faber S. M., Jackson R. E. 1976, ApJ, 204, 668
- Faber S. M., Tremaine S., Ajhar E.A. et al. 1997, AJ 114, 1771
- Ferrarese L., Côté P., Jordán A. et al. 2006, ApJS 164, 334
- Fukugita M., Shimasaku K., Ichikawa T. 1995, PASP 107, 945
- Geha M., Guhathakurta P., van der Marel R. P., 2003, AJ, 126, 1794
- Graham A. 2002, ApJ 568, L13
- Graham A. & Guzmán R. 2003, AJ 125, 2936
- Joseph C. L., Merritt D., Olling R. et al. 2001, ApJ, 550, 668
- Kormendy J. 1977, ApJ 218, 333
- Le Borgne D., Rocca-Volmerange B., Prugniel P. et al. 2004, A&A 425, 881
- Lisker T., Grebel E.K., Binggeli B. 2006, AJ 132, 497
- Lisker T., Grebel E.K., Binggeli B., Glatt K. 2007, astro-ph/0701429
- Matteucci F., 1994, A&A, 288, 57
- Mieske S., Infante L., Hilker M. et al. 2005, A&A 430, L25

- Nieto J.-L. & Prugniel P. 1987, A&A 186, 30  
Paturel G., Petit C., Prugniel P. et al. 2003, A&A 412, 45  
Rose J.A., Arimoto N., Caldwell N. et al. 2005, AJ 129, 712  
Sánchez-Blázquez P., Gorgas J., Cardiel N., González J. 2006, A&A 457, 809  
Schlegel D.J., Finkbeiner D.P., Davis M. 1998, ApJ 500, 525  
Sil'chenko O. K. 2006, ApJ 641, 229  
Stiavelli M. Miller B.W., Ferguson H.C. et al. 2001, AJ 121, 1385  
Thomas D., Maraston C., Bender R. 2003, MNRAS 339, 897  
van der Marel R.P., Cretton N., de Zeeuw P.T., Rix H.-W. 1998, ApJ, 493, 613  
van Zee L., Skillman E., Haynes M. 2004, AJ, 128, 121  
Worthey G., Faber S. M., González J.J., Burstein D. 1994, ApJS 94, 687  
Ziegler B. L. & Bender R. 1998, A&A 330, 819